Graphical Abstract

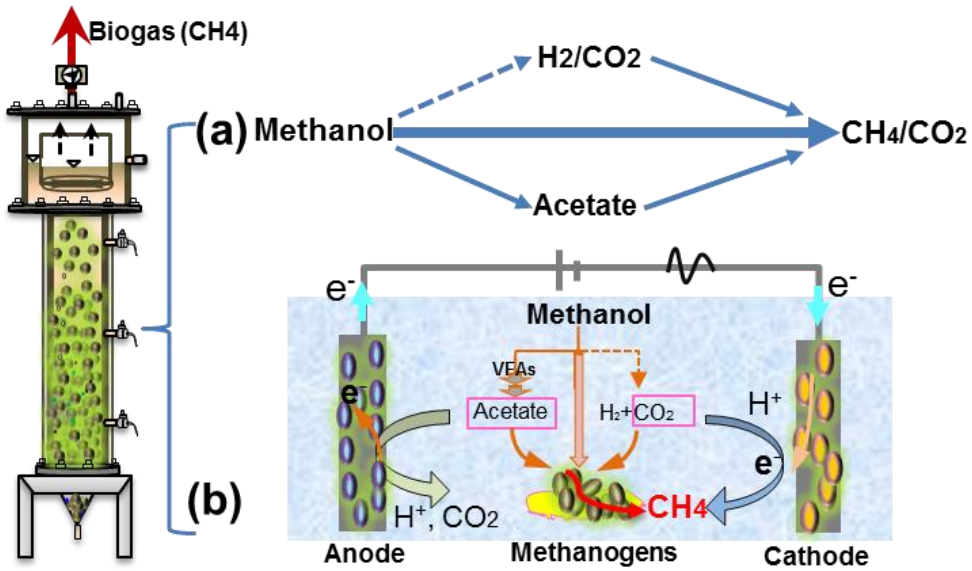

Research Highlights:

- Potential of MEC to upgrade methanolic wastewater treatment in UASB reactor was evaluated.
- Use of MEC improved methane production by around 10.1%.
- Bioelectrochemical process reinforced EPS secretion and formation of $[\text{-Fe-EPS-}]_n$ matrix.
- Bioelectrochemical process diversified microbial compositions and recycled wasted CO_2.

Continuous micro-current stimulation to upgrade methanolic wastewater biodegradation and biomethane recovery in an upflow anaerobic sludge blanket (UASB) reactor

Guangyin Zhen [a,b], Xueqin Lu [c,*], Takuro Kobayashi [b], Lianghu Su [d], Gopalakrishnan Kumar [e], Péter Bakonyi [f], Yan He [a], Periyasamy Sivagurunathan [b], Nándor Nemestóthy [f], Kaiqin Xu [b,*], Youcai Zhao [g]

a. Shanghai Key Lab for Urban Ecological Processes and Eco-Restoration, School of Ecological and Environmental Sciences, East China Normal University, Dongchuan Rd. 500, Shanghai 200241, PR China

b. Center for Material Cycles and Waste Management Research, National Institute for Environmental Studies, 16-2 Onogawa, Tsukuba, Ibaraki 305-8506, Japan

c. Department of Civil and Environmental Engineering, Graduate School of Engineering, Tohoku University, Sendai, Miyagi 980-8579, Japan

d. Nanjing Institute of Environmental Sciences of the Ministry of Environmental Protection, 210042, Nanjing, PR China.

e. Department of Environmental Engineering, Daegu University, Jillyang, Gyeongsan, Gyeongbuk, Republic of Korea

f. Research Institute on Bioengineering, Membrane Technology and Energetics, University of Pannonia, Egyetem ut 10, 8200 Veszprém, Hungary.

g. The State Key Laboratory of Pollution Control and Resource Reuse, Tongji University, Shanghai 200092, PR China.

***Corresponding author:** Xueqin Lu

Tel.: 81-29-850-2339

Fax: 81-29-850-2560

E-Mail address: zhenguangyin@163.com; luxueqin0220@126.com; joexu@nies.go.jp

Abstract

The dispersion of granules in upflow anaerobic sludge blanket (UASB) reactor represents a critical technical issue in methanolic wastewater treatment. In this study, the potentials of coupling a microbial electrolysis cell (MEC) into an UASB reactor for improving methanolic wastewater biodegradation, long-term process stability and biomethane recovery were evaluated. The results indicated that coupling a MEC system was capable of improving the overall performance of UASB reactor for methanolic wastewater treatment. The combined system maintained the comparatively higher methane yield and COD removal efficiency over the single UASB process through the entire process, with the methane production at the steady-state conditions approaching 1504.7 ± 92.2 mL-CH_4 L^{-1}-reactor d^{-1}, around 10.1% higher than the control UASB (i.e. 1366.4 ± 71.0 mL-CH_4 L^{-1}-reactor d^{-1}). The further characterizations verified that the input of external power source could stimulate the metabolic activity of microbes and reinforced the EPS secretion. The produced EPS interacted with $Fe^{2+/3+}$ liberated during anodic corrosion of iron electrode to create a gel-like three-dimensional [-Fe-EPS-]$_n$ matrix, which promoted cell-cell cohesion and maintained the structural integrity of granules. Further observations via SEM and FISH analysis demonstrated that the use of bioelectrochemical stimulation promoted the growth and proliferation of microorganisms, which diversified the degradation routes of methanol, convert the wasted CO_2 into methane and accordingly increased the process stability and methane productivity.

Keywords: Upflow anaerobic sludge blanket (UASB); Methanol; Microbial electrolysis cell (MEC); Electromethanogenesis; Extracellular polymeric substances (EPS)

1. Introduction

Shortage of global energy continues to be intensified because of the rapid industrialization and urbanization. Intensive consumption of carbon-based fossil fuel has forced the scientists to search for sustainable energy alternatives. Harvest and utilization of chemical energy from a myriad of waste streams represents a popular and of great promise research direction and will play a role in global energy security. As predicated by International Energy Agency (IEA) (IEA, 2016), the uptake of renewable energy will reach 60% of the total power generated by 2040. In order to recover as much renewable energy as possible from waste sources, numerous efforts have been dedicated to the development of various energy-efficient anaerobic treatment technologies, such as upflow anaerobic sludge blanket (UASB) (Li et al., 2011; Lu et al., 2015), anaerobic submerged membrane bioreactor (AnSMBR) (Gouveia et al., 2015), etc. Of them, upflow anaerobic sludge blanket (UASB), as a well-established process, has been universally applied in various real wastewater treatment for several decades, which cannot only covert chemical energy in soluble organics present in wastewaters to value-added bioenergy but synchronously realize wastewater purification. One of the available renewable energy reservoirs can be methanolic wastewater, an evaporator condensate with substantial energy and resource potential from the Kraft pulping process (Bhatti et al., 1996). The scientific research upon methanolic wastewater treatment by means of UASB has been initiated since late 1970s (Lettinga et al., 1979), however, until recently the potential of this approach to treat methanolic wastewater remains not clearly recognized and the long-term process stability still could not be guaranteed (Kobayashi et al., 2011; Lu et al., 2015).

Methanol is the simplest carbon source, but it sustains a complex web of biodegradation routs under anaerobic environments (Paulo et al., 2004). Methanol can be converted into methane either directly by methylotrophic methanogens or via intermediates such as acetate with the synergy of acetogens and acetoclastic methanogens (Florencio et al., 1997). The

long-term process stability of the reactor is closely related to the route used for methanol metabolism. If methanol biodegradation is accomplished via the former, high bioenergy recovery efficiency can be expected. In fact, this is the mostly observed scenario in methanolic wastewater treatment especially when methanol is the major carbon source. However, such system always accompanies with severe granules rupture because of excessively simple microbial community, which can induce granules washout and cause process upset and instability (Lu et al., 2015). On the other hand, the co-existence of the second rout can diversify microbial community and relieve this problem to a certain degree; however, the main issue for this scenario is acetate accumulation as a result of slow growth rate of acetoclastic methanogens as well as their high susceptibility to environment. Acetate accumulation in turn leads to pH drop, and consequently, impairs the reactor performance (Florencio et al., 1996; Lin et al., 2008). For reducing granular disintegration, various attempts have been examined, including the addition of starch (Kobayashi et al., 2011) or sulfate (Lu et al., 2017) with the purpose of diversifying microorganisms entrapped within granules, or elevating influent Ca^{2+} concentration (Lu et al., 2015) to accelerate the formation of three-dimensional [-Ca-EPS-]$_n$ network, facilitating sludge granulation. The commonly used strategy to tackle volatile fatty acids (VFAs) accumulation is alkalinity supplementation, which creates favorable pH conditions for methanogenesis but consumes a great amount of bicarbonates ($NaHCO_3$) (Florencio et al., 1995; Florencio et al., 1996).

Microbial electrolysis cell (MEC) is a newly developed biotechnological device and nowadays are receiving worldwide attention for a wide variety of electrofuels production as well as wastes biorefinary. In a such system, the electroactive biofilms enriched at anode surface oxidize organic substances (mainly acetate) into bicarbonate and protons and liberate electrons (Selembo et al., 2009); the electrons by the assistance of a small external power are driven to the cathode and combine with protons to generate H_2 (i.e. electrohydrogenesis)

(Rozendal et al., 2007; Wagner et al., 2009), or with carbon dioxide to form multi-carbon biofuels such as methane (i.e. electromethangenesis) (Villano et al., 2010; Zhen et al., 2016). Because of the outstanding features, MEC system has been modified and combined with several anaerobic processes for different purposes. The stimulatory effect on enhancing the performance and stability of the reactors has been indeed demonstrated in a number of MEC-combined anaerobic systems (Koch et al., 2015; Li et al., 2016; Zhen et al., 2016a). Shen et al. (2014) evidenced that the combination of a bioelectrochemical system with an UASB improved the *p*-nitrophenol removal. Zhao et al. (2014) also coupled the electromethanogenesis into an UASB reactor to improve anaerobic methanogenesis for high organic load rate acetate wastewater treatment, and they noted the beneficial role of anodic oxidization in degrading acetate, which reduced the risk of acetoclastic methanogens inhibition and maintained a stable performance. Thus, it can be imagined that if a MEC platform is integrated to the methanol-fed UASB, this could not only eliminate acetate accumulation and enhance methane conversion but also purify biogas through the electroreduction of carbon dioxide. To date, the available information associated with the application of UASB-MEC combined system for methanolic wastewater anaerobic treatment is still very limited.

Therefore, the present study aimed at exploring the potentials of coupling a MEC into an UASB reactor for improving methanolic wastewater biodegradation, long-term process stability and biomethane recovery. Scanning electron microscope (SEM) was used to visualize the microstructure of the granules developed with or without MEC's participation. Additionally, Fluorescence *in-situ* hybridization (FISH) has been carried out to analyze the possible effects of bioelectrochemical stimulation on microbial communities.

2. Material and methods

2.1. Methanolic wastewater and seed inoculum

According to the chemical components of real methanolic wastewater, the synthetic wastewater was prepared and used as the influent in continuous experiments. The synthetic wastewater contained (mg L^{-1}): 13300 COD (7600 methanol + 555 sucrose), 1500 $NaHCO_3$, 750 $Na_2S{\cdot}9H_2O$, 850 NH_4Cl, 250 K_2HPO_4, 100 KH_2PO_4, 309 $C_5H_5Na_3O_7{\cdot}2H_2O$, 263.3 $CaCl_2{\cdot}2H_2O$, 1.4 $CoCl_2{\cdot}6H_2O$, 1.1 $CuCl_2{\cdot}2H_2O$, 625 $FeCl{\cdot}4H_2O$, 122 $MgCl_2{\cdot}6H_2O$, 3.2 $MnCl_2$, 2.7 $NiCl_2{\cdot}6H_2O$, 5.2 $ZnCl_2$, 0.5 $NaMoO_4{\cdot}2H_2O$, and 74.4 $AlCl_3{\cdot}6H_2O$. The initial pH of the medium was adjusted into 7.0 with 0.1 NaOH or H_2SO_4.

The seed inoculum used in this investigation was collected from an existing 6-L methanol-fed UASB reactor in Tohoku University, Japan; the reactor has been operated in continuous mode for roughly one year with methanol as the sole carbon source. Methanol concentration (3.0–15.0 g-COD L^{-1}) varied at different phases according to the required organic loading rates. Throughout the entire period, $NaHCO_3$ was added at a concentration of 1500 mg L^{-1} to ensure pH stability. The methanogenic activity measured with methanol as the substrate was 1.32–2.11 g-COD_{CH4} g^{-1}-VSS d^{-1}. More details for cultivating the seed inoculum, readers are referred to Lu et al. (2015). The granular sludge was allowed to settle overnight, the supernatant was discarded and 150 g of the wet sludge was inoculated into each of the reactors, occupying approximately one third of the total working volume.

2.2 Reactor construction and experimental design

Two lab-scale UASB reactors, made of polyvinyl chloride, were fabricated with a tubular section at the bottom and an expanded section termed as gas-liquid-solid separator (GLSS) at the top. These reactors were operated with a hydraulic retention time (HRT) of 48 h at a temperature controlled at 35 ˚C throughout the whole experiments (Fig. 1). The reactors had a working volume of approximately 500 mL each, with the inner diameter of 5 cm and the

reaction zone height of 24 cm. The influent was fed from the bottom of the rectors by the peristaltic pump (MP-1000, Tokyo Rikakiki Co., Ltd, Japan). Three equidistant ports along reactor height were provided to facilitate sampling. The two reactors were operated under identical operational conditions, except for the input of external micro-current stimulation. One reactor (hereafter referred to as UASB-MEC) was supplemented with a low external power: 0.4 V during the first 120 days and then 0.6 V until the termination of the test; whereas for the purpose of comparison, no current was supplied to the second one (hereafter referred to as UASB), which acted as the control.

In the UASB-MEC reactor, anode was a pair of iron sticks (φ80 mm × 200 mm, RDOC8-200, LMS, Japan), which was fixed in parallel onto the inside wall of the reactor. The helical compression spring cathode (DC671, Accurate Inc., Japan) was made of grade SAE1080, which has the chemical compositions: 0.74–0.88% C, 0.15–0.30% Si, 0.60–0.90% Mn, < 0.040% P, and < 0.050% S (balance Fe). The helical cathode (2.5 mm wire diameter, 24 cm length and 2.75 cm outside diameter) as the working electrode was installed in the center of the reactor to be situated in the sludge bed. Prior to use, the electrode materials were washed with diluted HCl and then deionized water to clean their surfaces. The electrodes were then connected through a titanium wire that extended through the rubber stopper to a regulated digital DC power supply (AD-8735, A&D Co., Japan) for controlling the electrical voltage. A digital multi-meter (Model: PC720M, Sanwa Electric Instrument Co., Ltd., Tokyo, Japan) was used to measure and register the voltage as a function of time across a 10 Ω resistor (Artec, Japan) incorporated in the electrical circuit as time, and the current was then calculated via Ohm's law (i.e. $I = U/R$).

Fig. 1.

148 ***2.3 Analytical methods***

149 Total solids (TS) and volatile solids (VS) were analyzed following Standard Methods (APHA,
150 1998). The pH was determined using a HORIBA Compact pH meter (B-212, Japan). Total
151 chemical oxygen demand (TCOD) and soluble chemical oxygen demand (SCOD) were
152 measured using COD Digest Vials (HACH, Loveland, CO, USA) in accordance with the
153 manufacturer's instructions. Percentages of H_2, CH_4, CO_2 and N_2 in the produced biogas were
154 analyzed using a gas chromatograph (GC-8A, Shimadzu, Japan) equipped with a thermal
155 conductivity detector (TCD, 80 mA) and a 2 m stainless steel column packed with Shicarbon
156 ST (Shimadzu GLC). The concentrations of individual VFAs including acetic, propionic, *iso*-
157 butyric, *n*-butyric, *iso*-valeric and *n*-valeric acids were determined by a gas chromatograph
158 (GC14B, Shimadzu, Japan) equipped with a flame ionization detector (FID) using helium as
159 carrier gas (50 kPa) and a StabiliwaxR-DA capillary column (Restek, Bellefonte, PA, USA).
160 Extracellular polymeric substances (EPS, including slime EPS (S-EPS), loosely bound EPS
161 (LB-EPS) and tightly bound EPS (TB-EPS)) were extracted from granules according to the
162 method described by Zhen et al. (2013). Protein (PN) in extracted EPS was determined by the
163 modified Lowry procedure (Frolund et al., 1996), and polysaccharide (PS) was stained with
164 the phenol-sulfuric acid method (Dubois et al., 1956).

165 The granules developed with or without the integration of MEC were sampled for
166 scanning electron microscope (SEM) observation. The procedures for sample preparation and
167 SEM analysis were described in details in our previous publications (Zhen et al., 2014, 2015).
168 Besides, the part of the granules sampled from the reactors (ultrasonication at 60 W for 5 min)
169 were subjected to Fluorescence *in-situ* hybridization (FISH) analysis. The samples were
170 pretreated according to Zhen et al. (2016b, 2016c). Fluorescence labels of the oligonucleotide
171 probes used here included ARC915 (*Archaea*, GTGCTCCCCCGCCAATTCCT) (Raskin et
172 al., 1994) and EUB338 (Bacteria, GCTGCCTCCCGTAGGAGT) (Daims et al., 1999). After

hybridization, the cells suspensions on slides were stained with 4, 6-diamidino-2-phenylindole (DAPI) and observed via an Eclipse E1000 research-level microscope (Nikon, Japan) equipped with a HAMAMATSU ORCA-ER digital camera and a computer-based image analysis system (AQUA-Lite software).

2.4 Statistical analysis

Analysis of variance (ANOVA) was performed using Microsoft Excel 2013 to determine statistical differences in the results obtained from different conditions.

3. Results and Discussion

3.1. Current and methane production

Fig. 2 shows the time course of current values, and methane content and production rate. Current density is a useful parameter directly reflecting the microbial metabolic dynamics in bioelectrochemical system. At the poised voltage of 0.4 V, current values changed greatly (6.4 ± 1.3 mA) during the initial period (i.e. start-up) (Fig. 2a), and they started to become stabilized from day 70 onward, being on average 5.3 ± 0.6 mA. This observation reflected that the electroactive biofilms able to release and accept electrons had been successfully enriched and colonized on the electrode surface. Then when the applied voltage was further increased to 0.6 V, the conspicuous current variation resumed even though the current values were magnified (6.6 ± 0.9 mA). This indicated that the voltage of 0.6 V might be too high in this situation, which suppressed the metabolisms and activities of electroactive biofilms, changed and even broke the previously established electrochemically dynamic equilibriums (at 0.4 V), and accordingly caused the process upset and instability. This is in accordance with the findings of Ding et al. (2016), who noticed the cell rupture (indicated by lactic dehydrogenase, LDH) and sharply inhibited metabolic activities (indicated by adenosine triphosphate, ATP) in bioanode and biocathode when too high voltage was adopted (> 0.8 V

198 in their study). Besides, high levels of voltage would also bring the negative effects on the
199 native-born microbes in granules by changing cell surface properties (Luo et al., 2005),
200 thereby further aggravating the process upsets and instability.

201 Methane production showed highly instable during the start-up phase, irrespective of the
202 voltage (Fig. 2b and c). Nonetheless, the input of external power notably upgraded the
203 methane productivity of methanol (*P*-value ≈ 0.05). The UASB-MEC reactor produced an
204 average 1835.0 ± 417.0 mL-CH_4 L^{-1}-reactor d^{-1} with an average CH_4 content of 79.0 ± 3.1%
205 during the initial 70 days, whereas it was 1615.2 ± 310.7 mL-CH_4 L^{-1}-reactor d^{-1} (75.3 ±
206 7.9%) for single UASB process. Both reactors entered the steady-state phase (i.e. day 70–120)
207 from then on. The UASB-MEC reactor during this period showed significantly improved
208 bioenergy production performance (*P*-value = 2.57×10^{-5} << 0.01), i.e. 1504.7 ± 92.2 mL-
209 CH_4 L^{-1}-reactor d^{-1}, roughly 10.1% higher than the control UASB (i.e. 1366.4 ± 71.0 mL-
210 CH_4 L^{-1}-reactor d^{-1}). These observations correlated well with those reported by Zhen et al.
211 (2016a), Guo et al. (2016), Cai et al. (2016), Sasaki et al. (2011), Koch et al. (2015), and
212 Batlle-Vilanova et al. (2015), who independently identified the stimulatory influences of
213 power input on methanogenesis of waste organics. Likewise, Marone et al. (2016)
214 constructed a similar system with halophilic consortium as biocatalysts to treat recalcitrant
215 table olive brine processing wastewater (TOPW) and reported a maximum methane yield of
216 701 ± 13 NmL-CH_4 L^{-1}-TOPW with up to 80% of phenolic (i.e. hydroxytyrosol and tyrosol)
217 removal at an anodic potential of +0.2 V vs. SCE; comparatively, nearly no methane was
218 detected in single anaerobic digester. They noted that the specific enrichment of electroactive
219 microorganisms (i.e. genera *Desulfuromonas* and *Geoalkalibacter*) benefited the TOPW
220 oxidation and biomethane generation.

221 From day 120 on, the performance of control UASB process became deteriorated, and
222 the serious granule rupture and washout took place. Methane production fluctuated in a wide

range of 624.6–1548.9 mL-CH_4 L^{-1}-reactor d^{-1} (i.e. 1251.2 ± 310.6 mL-CH_4 L^{-1}-reactor d^{-1}). Many previous works have also noticed the similar symptoms during the long-term anaerobic treatment of methanolic wastewater (Nishio et al., 1993; Kobayashi et al., 2011; Lu et al., 2015, 2017), and Lu and co-workers attributed this to several biotic/abiotic factors: (i) depletion of extracellular polymeric substances (EPS); (ii) restricted formation of hard core and weak $Me^{2/3+}$-EPS bridge effect; and (iii) simplification of microbial community with methanol acclimation (Lu et al., 2015). In this regard, until the termination of the experiments, methane production did not recover. The inherent technical issues have thus restricted the widespread applications of UASB technology in real methanolic wastewater. In sharp contrast, the UASB-MEC reactor maintained highly stable levels of methane production until day 135 (i.e. 1559.0 ± 157.6 mL-CH_4 L^{-1}-reactor d^{-1}), and then an abrupt variation was detected during the latter phase, presumably attributable to the fact that high voltage might lead to cell rupture and plasmatorrhexis (Wang et al., 2017), and subsequently induced the process upsets. As stressed by Ding et al. (2016), when the applied voltage was increased from 0.8 to 1.0 V, the metabolism activity of microbes indicated by adenosine triphosphate (ATP) decreased by 27% in anode while 46% in cathode, and it decreased by up to 55% and 66% respectively when the voltage was 2.0 V. Nonetheless, because of comparatively low voltage (~0.6 V) poised in the present study, the reactor performance was hardly affected, and the average methane production reached up to 1679.2 ± 307.1 mL-CH_4 L^{-1}-reactor d^{-1}, approximately 29.3% higher than that obtained from the UASB alone. Moreover, during the entire process, methane content in the biogas produced from UASB-MEC reactor was always higher than that from the control UASB process (i.e. 79.8 ± 2.1% vs 76.7 ± 4.7%; *P*-value = $9.69 \times 10^{-7} << 0.01$) (Fig. 2b). These observations strongly confirmed the beneficial roles of bioelectrochemical system in improving waste methanogenesis efficiency. Considering the

potential instability and upsets caused by high voltage, the imposed voltage of below 0.6 V is suggested in a methanol-fed UASB process for a safe and stable operation.

Fig. 2.

3.2. Physiochemical properties of effluent

The basic properties of treated effluent in terms of pH, TS, VS, and COD are illustrated in Fig. 3. The electric stimulation was applied, yet no considerable difference in pH values was detected during the whole process (*P*-value = 0.2945), possibly because of sufficient alkalinity ($NaHCO_3$) provided in the influent. They both fell within the pH level suitable for methanogenesis (i.e. 6.5–8.0) (Fig. 3a). Granule washout, as noted before, is the vital factor constricting the application of UASB process in real methanolic wastewater treatment. However, this seems have been controlled effectively by coupling an MEC platform (*P*-value-TS = $3.98 \times 10^{-46} << 0.01$; *P*-value-VS = $3.31 \times 10^{-41} << 0.01$). The UASB-MEC reactor when operated at 0.4 V presented lower TS and VS values of 2.05 ± 0.13 mg L^{-1} and 0.32 ± 0.11 mg L^{-1} during the steady-state condition, as compared to 2.21 ± 0.12 mg L^{-1} and 0.36 ± 0.14 mg L^{-1} measured from the control UASB, respectively (Fig. 3b and c). At the voltage of 0.6 V, despite the occurrence of occasional instability, TS and VS from the integrated system still kept particularly lower than those of the control UASB, indicating the favorable influence of electric stimulation. Likewise, TCOD and SCOD in the effluent followed the similar profile (Fig. 3d and e). For instance, the average effluent TCOD in single UASB process maintained at 205.02 ± 65.02 mg L^{-1} between day 70 and 170, with the corresponding removal efficiency being $98.5 \pm 0.5\%$; comparatively, it decreased to 147.06 ± 50.84 mg L^{-1} (*P*-value = $1.88 \times 10^{-4} < 0.01$) when the UASB-MEC reactor was utilized, and its removal efficiency approached up to $98.9 \pm 0.4\%$. The higher COD removal, the more bioenergy conversion, in accordance to the CH_4 production pattern. The relieved sludge

washout and improved performance might be mainly explained by two reasons: (i) the growth and formation of electroactive microorganisms and resultant diversification of microbial community, and (ii) the liberation of Fe ions from iron stick anode during anodic oxidization, which provoked the secretion of extracellular polymeric substances (EPS) and formation of three dimensional [-Fe-EPS-]$_n$ matrix, thereby helping capture the small size particles and develop the compact granules (Lu et al., 2015, 2017). Besides, precipitation of Fe ions with sulfide could also form iron-sulfide particles, which further favored cells adherence and granule development. The beneficial effects of element Fe on sludge granulation were also highlighted by Yu et al. (2000), Vlyssides et al. (2009), Liu et al. (2011a), and recently by Lu et al. (2017). Most of the previous studies usually use iron ions ($Fe^{2+/3+}$); comparatively speaking, the employment of solid iron electrode in this study possesses multiple advantages over the conventional iron ions since it cannot only supply the Fe required but also serve as the conductive carrier for the rapid growth and acclimation of electroactive bacteria with the assistance of electrochemical stimulation. All of these factors eventually boosted the overall performance of UASB reactor. Obviously, the combination of UASB with an MEC equipped with iron electrode opens up an avenue and new opportunities for highly efficient treatment of methanolic wastewater and simultaneous chemical energy harvesting.

Fig. 3.

3.3. Underlying enhancing mechanisms in the combined UASB-MEC system

3.3.1. EPS secretion and contribution to sludge granulation

EPS, secreted by the multispecies community of microorganisms under certain environmental conditions, are a major compound of anaerobic granules and play an important role in

maintaining the integrality and mechanical strength of granules and the long-term stability of the reactor. EPS can be divided into three parts, i.e. S-EPS, LB-EPS and TB-EPS, based on their different location in granules (Li and Yang, 2007; Zhen et al., 2012b, 2013). Three types of EPS were separated and quantified at the end of experiments, and the corresponding results are depicted in Fig. 4. As can be seen, the electrochemical stimulation clearly promoted the secretion of granular EPS, in particular LB-EPS and TB-EPS. They both increased to 6.05 ± 0.84 mg g^{-1}-VS and 9.72 ± 1.32 mg g^{-1}-VS, in contrast to 4.60 ± 1.03 mg g^{-1}-VS and 7.00 ± 2.01 mg g^{-1}-VS extracted from the control UASB reactor, respectively. Moreover, granular flocs grown in the UASB-MEC system contained more TB-EPS and less LB-EPS (LB-/TB-EPS = 0.62) whereas the granules derived from the single UASB reactor had more LB-EPS and less TB-EPS (LB-/TB-EPS = 0.66). It is universally accepted in the literature that LB-EPS, especially TB-EPS, are the decisive factor governing flocs flocculation and sludge granulation process, whereas the effect of S-EPS is negligible. S-EPS are evenly distributed in the liquid phase, LB-EPS, located in the outer layer of granules, extend from the TB-EPS with a highly porous and dispersible structure, and TB-EPS, located in the core region of the granules, are highly compact and rigid (Li and Yang, 2007; Liu et al., 2010; Zhen et al., 2012a, 2013). As such, the contribution of each EPS fraction to sludge granulation differs with their spatial location inside the granules (Liu et al., 2010). LB-EPS are able to aid in the formation of the three-dimensional gel-like network that keeps cells together and causes small particles capture and flocculation; TB-EPS can further firmly pack the aggregated cells and inert particles through strong physiochemical interactions, thereby resulting in better granulation and a more tightly compact structure. This appears to be the core reason for the stabilized process observed in the UASB-MEC system. The similar outcomes were also documented by other researchers (Zhou et al., 2007; Lu et al., 2015, 2017).

The contribution of each EPS was further detailed when the protein/polysaccharide ratio (PN/PS ratio) was calculated on different EPS fractions (Fig. 4). The two granule samples contained a much higher fraction of protein, no matter in S-EPS, LB-EPS or TB-EPS, agreeing well with our previous observations (Lu et al., 2015, 2017). Similarly, Ismail et al. (2010) also quantified the EPS compositions for granules from UASB reactors fed with high sodium concentration wastewaters, and found protein to be the most abundant compound (around 87% and 94%). The electrochemical stimulation that was applied in this study affected the EPS composition and considerable difference in PN/PS ratio of total EPS was observed in the granules from the two reactors. Granular flocs developed in the UASB-MEC system exhibited higher quantities of protein in its total EPS (i.e. LB-EPS + TB-EPS) fraction (PN/PS ratio = 4.98) compared to the granules derived from the single UASB reactor (PN/PS ratio = 4.06). This result implied that the input of electric current stimulated the metabolic activity of microbes and reinforced the protein secretion. Higher amount of protein has been hypothesized to play a central role in stabilizing granular structure (McSwain et al., 2005). This is because in comparison with hydrophilic polysaccharide polymers that absorb water or biological fluids, protein has a high content of negatively charged amino acids and thus it is more involved in electrostatic bonds with multivalent cations (e.g. Ca^{2+}, $Fe^{2/3+}$, Al^{3+}, etc.) to act as a bridge between the components, promoting bacterial aggregation (Laspidou and Rittmann, 2002; Basuvaraj et al., 2015). In this context, protein interacted with $Fe^{2+/3+}$ released during anode corrosion reaction to create a rigid, non-deformable $[\text{-Fe-EPS-}]_n$ matrix, which promoted cell-cell interaction and cohesion and eventually maintained the process stability of the reactor. This is consistent with Basuvaraj et al. (2015) who reported that granular flocs that contained high faction of protein possessed more closely packed cells; in comparison, the flocs with high quantities of polysaccharide were mainly composed of loosely compacted cells. The beneficial roles of Fe^{2+} were also documented by Kobayashi et

348 al. (2015), who noticed that Fe^{2+} supplementation might reduce EPS elution through forming
349 Fe^{2+}-bound EPS matrix and enhance granules stability.
350
351 **Fig. 4.**
352
353 3.3.2. Morphological characteristics of granular flocs
354 The morphological appearance of granules grown with electrochemical stimulation in the
355 UASB-MEC system was analyzed through SEM and compared with those from the single
356 UASB reactor (Fig. 5 and Fig. S1 in Supporting Information). There was striking difference
357 in the microstructure of the two granules. The single UASB showed severe granule
358 disintegration and the granules in this case were highly dispersed, irregular, and weak with an
359 open exterior surface where microbial cells were loosely compacted (Fig. 5a). The fragile
360 texture possesses very low resistance to external turbulence, and thereby could be easily
361 disassociated into small flocs. This explained the serious sludge dispersion and wash-out
362 occurring in the UASB reactor. Comparatively, the granules enriched in the UASB-MEC
363 system were obviously larger in size, intact, and firm (Fig. 5b). A further close-up of this
364 structure revealed that a higher amount of EPS-like matrix were produced and accumulated
365 onto the surface of granules. The thick layer of polymeric gel-like network held microbial
366 cells together tightly by chemical cross-linking and physical entanglement (Mikkelsen and
367 Keiding, 2002), thereby reducing the degree of dispersion and reinforcing the structural
368 integrity of anaerobic granules. Unfortunately, at present, the descriptions associated with the
369 influence of electrochemical stimulation on sludge granulation are yet too few in the
370 literature (Liu et al., 2011b), and thus this hinders any meaningful comparisons. The current
371 work represents a preliminary scientific attempt, and more efforts are still highly required in
372 this field. Apart from the substantial improvement in sludge granulation, the EPS will also

hold up an umbrella for anaerobes entrapped within the granules, which is thought to increase their resistance and adaptability to harsh external environmental conditions (Guibauda et al., 2012; Lu et al., 2017).

Fig. 5.

3.3.3. Fluorescence *in-situ* hybridization (FISH) analysis

To in-depth elucidate the favorable stimulation of external power supply on the reactor process stability and biomethane recovery, the FISH analysis was further used to analyze the special microbial composition of the granules (Fig. 6 and Fig. S2 in Supporting Information). Hybridizing with Cy3-labeled oligonucleotide probe ARC915 and EUB338 targeted the presence of the domain *Archaea* and *Bacteria*, respectively. The numbers of both *Archaea* and *Bacteria* showed an insignificant but still appreciable increase in the combined UASB-MEC system, due to the introduction of external power source, in good agreement with the SEM results (Fig. 5). One possible reason for the increased microbial abundance might be associated to the liberation of Fe ions from anode corrosion, which stimulated the synthesis of key enzymes and proliferation of the anaerobes, e.g. pyruvate-ferredoxin oxidoreductase (POR) which contains Fe-S clusters and plays an important role in acidogenesis (Liu et al., 2012), or cytochrome and ferredoxin in methylotrophic methanogens (Shen et al., 1993). This finding is coincident with those reported by Liu et al. (2011b) who observed the significant rise in methanogens when an electric field (1.2–1.3 V) was applied in a built-in zero valent iron-UASB reactor, and by Zhen et al. (2016a), who noted that the use of a small external power could enrich *Archaea* in an *Egeria densa*-fed MEC-AD reactor, contributing greatly to the process stability and bioenergy recovery. *Archaea* represent the methanogens and the detected *Bacteria* are mainly associated with fermentative bacteria, or homoacetogens. It is

well-known that methanol can be anaerobically decomposed via three routes: (i) direct methylotrophic ($4CH_3OH \rightarrow 3CH_4 + CO_2 + 2H_2O$, $\Delta G^{0'} = -315$ kJ mol^{-1}), (ii) acetoclastic ($4CH_3OH + 2H_2CO_3 \rightarrow 3CH_3COOH + 4H_2O$, $\Delta G^{0'} = -222$ kJ mol^{-1}; $CH_3COOH + H_2O \rightarrow CH_4 + H_2CO_3$, $\Delta G^{0'} = -31$ kJ mol^{-1}), and (iii) hydrogenotrophic methanogenesis ($CH_3OH + H_2O \rightarrow 3H_2 + H_2CO_3$, $\Delta G^{0'} = +23$ kJ mol^{-1}; $CH_3COOH + 4H_2O \rightarrow 4H_2 + 2H_2CO_3$, $\Delta G^{0'} = +95$ kJ mol^{-1}; $CO_2 + 4H_2 \rightarrow CH_4 + 2H_2O$, $\Delta G^{0'} = -136$ kJ mol^{-1}) (Paulo et al., 2003, 2004; Lu et al., 2015). High abundance of fermentative bacteria could further drive the acidification of methanol while the increased methanogens ensured direct methylotrophic methanogenesis (route i) or the metabolism of VFAs and subsequent acetoclastic methanogenesis (route ii) at faster rates. As a result of this, the enhanced organics removal efficiency and higher methane productivity were sustained. Note that the bioconversion of methanol via route iii will be difficult occur in a normal UASB system because of unfavorable thermodynamics. Slightly different from our observations, Zhang et al. (2015), with the help of real-time PCR analysis, found that coupling of a bioelectrochemical system in anaerobic digesters increased the numbers of *Archaea* (from 0.64×10^8 to 1.36×10^8 copies ng^{-1}-DNA), but at the same time caused the reduction in *Bacteria* (from 2.62×10^9 to 1.43×10^9 copies ng^{-1}-DNA); even so, they still obtained the enhanced acidogenesis performance. The slight discrepancy is somewhat reasonable because of the differences in types of inoculum, physiochemical properties of substrates, operational conditions, etc.

Besides the uplifting effects on metabolic activities of granules, the UASB-MEC system with the input of a small power source also showed the potential to promote the methane conversion of methanol by means of bioelectrochemical reactions occurring on the surfaces of two electrodes. This process required the anodic oxidation of acetate by the enriched exoelectrogens and subsequent electromethanogenesis of CO_2 by electrotrophs on the cathode through combining with the electrons delivered from the anode (Fu et al., 2015; van Eerten-

Jansen et al., 2015). Due to the fact that there were no signs of acetate detected in both reactors regardless of the voltage, this retarded us to provide the direct evidence for the anodic oxidation of acetate. Nevertheless, CO_2 contents in the biogas produced from the UASB-MEC system were always lower than those in the single UASB process (Fig. S3 in Supporting Information), with the improved CH_4 productivity (Fig. 2b and c), indicating that the bioelectroreduction of CO_2 had indeed taken place. Batlle-Vilanova et al. (2015) applied a similar system for biogas upgrading, and they concluded that interspecies hydrogen transfer between *Clostridium* sp. and *Methanobacterium* sp., which combined the hydrogen produced with CO_2 to obtain methane, was the main mechanism for CO_2 electroreduction, and that the electromethanogenesis via direct electron transfer occurred to a minor extent. It is worth mentioning that the cathodic electrotrophs needed electrons from the anode to bioelectroreduce CO_2, which highlighted the possibility of the anodic oxidation of acetate to take place. Likewise, Zhao et al. (2014) documented that the uptake of electrons by cathodic acceptors was the major driving force for the acetate oxidation in the anode to happen. However, based upon the current data, it is still very difficult to quantify the relative importance of bioelectrochemical process in methanol degradation and methane production, and additional works are yet needed. Nonetheless, the integration of MEC with an UASB reactor cannot only upgrade organic degradation and methane productivity but also convert the wasted CO_2 into valued-added electrofuels and reduce greenhouse gas emission and as a consequence, this technology will play a role in environmental protection and global energy security in the near future. Besides, a simple schematic diagram was further drafted and are illustrated in Fig. 7 to provide a clearer map about the stimulatory roles of electrochemical stimulation in methanol metabolism and reactor process stability.

Fig. 6.

Fig. 7.

4. Conclusions

Coupling a MEC system showed the great potentials to stimulate the overall performance of UASB reactor for methanolic wastewater treatment. The combined systems maintained the comparatively higher methane yield and COD removal efficiency over the single UASB process through the entire process. The input of external power source stimulated the metabolic activity of microbes and reinforced the EPS secretion. The produced EPS could interact with $Fe^{2+/3+}$ released from iron stick anode during anodic corrosion reaction to create a rigid, three-dimensional $[\text{-Fe-EPS-}]_n$ matrix, which promoted cell-cell interaction and cohesion and eventually maintained the structural integrity of granules. Further observations via SEM and FISH analysis demonstrated that the use of bioelectrochemical stimulation promoted the growth and proliferation of microorganisms, which diversified the degradation routes of methanol, convert the wasted CO_2 into methane and accordingly increased the process stability and methane productivity. Additional efforts still should be made to quantify the relative role of bioelectrochemical process in methanol degradation and methane production.

Acknowledgements

The first author of this paper was supported by the postdoctoral fellowship (ID No. PU 14016) of the Japan Society for the Promotion of Science (Japan). The second author was supported by the postdoctoral fellowship (ID No.: P 16352) of the Japan Society for the Promotion of Science (Japan). Péter Bakonyi acknowledges the support received from National Research, Development and Innovation Office (Hungary) under grant number PD 115640.

References

APHA, 1998. Standard Methods for the Examination of Water and Wastewater, 20th ed, (Ed.) A.P.H. Association. Washington, DC, USA.

Basuvaraj, M., Fein, J., Liss, S.N., 2015. Protein and polysaccharide content of tightly and loosely bound extracellular polymeric substances and the development of a granular activated sludge floc. Water Res. 82, 104-117.

Batlle-Vilanova, P., Puig, S., Gonzalez-Olmos, R., Vilajeliu-Pons, A., Balaguer, M.D., Colprim, J., 2015. Deciphering the electron transfer mechanisms for biogas upgrading to biomethane within a mixed culture biocathode. RSC Adv. 5, 52243-52251.

Bhatti, Z.I., Furukawa, K., Fujita, M., 1996. Feasibility of methanolic waste treatment in UASB reactors. Water Res. 30, 2559-2568.

Cai, W.W., Han, T.T., Guo, Z.C., Varrone, C., Wang, A.J., Liu, W.Z., 2016. Methane production enhancement by an independent cathode in integrated anaerobic reactor with microbial electrolysis. Bioresour. Technol. 208, 13-18.

Daims, H., Brühl, A., Amann, R., Schleifer, K.H., Wagner, M., 1999. The domain-specific probe EUB338 is insufficient for the detection of all Bacteria: development and evaluation of a more comprehensive probe set. Syst. Appl. Microbiol. 22, 434-444.

Ding, A., Yang, Y., Sun, G., Wu, D., 2016. Impact of applied voltage on methane generation and microbial activities in an anaerobic microbial electrolysis cell (MEC). Chem. Eng. J. 283 260-265.

Dubois, M., Gilles, K.A., Hamilton, J.K., Rebers, P.A., Smith, F., 1956. Colorimetric method for determination of sugars and related substances. Anal. Chem. 28, 350-356.

Florencio, L., Field, J.A., Lettinga, G., 1995. Substrate competition between methanogens and acetogens during the degradation of methanol in UASB reactors. Water Res. 29, 915-922.

Florencio, L., Field, J.A., Lettinga, G., 1997. High-rate anaerobic treatment of alcoholic wastewaters. Braz. J. Chem. Eng. 14(4), https://dx.doi.org/10.1590/S0104-66321997000400016.

Florencio, L., Field, J.A., vanLangerak, A., Lettinga, G., 1996. pH-stability in anaerobic bioreactors treating methanolic wastewaters. Water Sci. Technol. 33, 177-184.

Frolund, B., Palmgren, R., Keiding, K., Nielsen, P.H., 1996. Extraction of extracellular polymers from activated sludge using a cation exchange resin. Water Res. 30, 1749-1758.

Fu, Q., Kuramochi, Y., Fukushima, N., Maeda, H., Sato, K., Kobayashi, H., 2015. Bioelectrochemical analyses of the development of a thermophilic biocathode catalyzing electromethanogenesis. Environ. Sci. Technol 49, 1225−1232.

Guibauda, G., Bhatia, D., dAbzac, P., Bourven, I., Bordas, F., Hullebusch, E.D.v., Lens, P.N.L., 2012. Cd(II) and Pb(II) sorption by extracellular polymeric substances (EPS) extracted from anaerobic granular biofilms: evidence of a pH sorption-edge. J. Taiwan. Inst. Chem. E. 43(3), 444-449.

507 Guo, Z., Thangavel, S., Wang, L., He, Z., Cai, W., Wang, A., Liu, W., 2017. Efficient methane
508 production from beer wastewater in a membraneless MEC with stacked cathode: the effect of
509 cathode-anode ratio on bioenergy recovery. Energ. Fuel. 31 (1), 615–620.
510 IEA, 2016. World Energy Outlook 2016 - Executive Summary.
511 http://www.iea.org/publications/freepublications/; 2016.
512 Ismail, S.B., de La Parra, C.J., Temmink, H., van Lier, J.B., 2010. Extracellular polymeric substances
513 (EPS) in upflow anaerobic sludge blanket (UASB) reactors operated under high salinity conditions.
514 Water Res. 44, 1909-1917.
515 Kobayashi, T., Xu, K.Q., Chiku, H., 2015. Release of extracellular polymeric substance and
516 disintegration of anaerobic granular sludge under reduced sulfur compounds-rich conditions. Energies
517 8, 7968-7985.
518 Kobayashi, T., Yan, F., Takahashi, S., Li, Y.Y., 2011. Effect of starch addition on the biological
519 conversion and microbial community in a methanol-fed UASB reactor during long-term continuous
520 operation. Bioresourc. Technol. 102, 7713-7719.
521 Koch, C., Kuchenbuch, A., Kretzschmar, J., Wedwitschka, H., Liebetrau, J., Müllera, S., Harnisch, F.,
522 2015. Coupling electric energy and biogas production in anaerobic digesters - impacts on the
523 microbiome. RSC Adv. 5, 31329-31340.
524 Laspidou, C.S., Rittmann, B.E., 2002. A unified theory for extracellular polymeric substances, soluble
525 microbial products, and active and inert biomass. Water Res. 36, 2711-2720.
526 Lettinga, G., Vandergeest, A.T., Hobma, S., Vanderlaan, J., 1979. Anaerobic treatment of methanolic
527 wastes. Water Res. 13, 725-737.
528 Li, J., Wang, J., Luan, Z., Deng, Y., Chen, L., 2011. Evaluation of performance and microbial
529 community in a two-stage UASB reactor pretreating acrylic fiber manufacturing wastewater.
530 Bioresour. Technol. 102, 5709-5716.
531 Li, X.Y., Yang, S.F., 2007. Influence of loosely bound extracellular polymeric substances (EPS) on
532 the flocculation, sedimentation and dewaterability of activated sludge. Water Res. 41, 1022-1030.
533 Li, Y., Zhang, Y., Liu, Y., Zhao, Z., Zhao, Z., Liu, S., Zhao, H., Quan, X., 2016. Enhancement of
534 anaerobic methanogenesis at a short hydraulic retention time via bioelectrochemical enrichment of
535 hydrogenotrophic methanogens. Bioresour. Technol. 218, 505-511.
536 Lin, Y., He, Y., Meng, Z., Yang, S., 2008. Anaerobic treatment of wastewater containing methanol in
537 upflow anaerobic sludge bed (UASB) reactor. Front. Environ. Sci. Eng. 2, 241-246.
538 Liu, X.M., Sheng, G.P., Luo, H.W., Zhang, F., Yuan, S.J., Xu, J., Zeng, R.J., Wu, J.G., Yu, H.Q.,
539 2010. Contribution of extracellular polymeric substances (EPS) to the sludge aggregation. Environ.
540 Sci. Technol. 44, 4355-4360.
541 Liu, Y., Zhang, Y., Quan, X., Chen, S., Zhao, H., 2011a. Applying an electric field in a built-in zero
542 valent iron--anaerobic reactor for enhancement of sludge granulation. Water Res. 45, 1258-1266.

Liu, Y., Zhang, Y., Quan, X., Li, Y., Zhao, Z., Meng, X., Chen, S., 2012. Optimization of anaerobic acidogenesis by adding Fe^0 powder to enhance anaerobic wastewater treatment. Chem. Eng. J. 192, 179-185.

Liu, Y.W., Zhang, Y.B., Quan, X., Chen, S., Zhao, H.M., 2011b. Applying an electric field in a built-in zero valent iron - Anaerobic reactor for enhancement of sludge granulation. Water Res. 45, 1258-1266.

Lu, X., Zhen, G., Chen, M., Kubota, K., Li, Y.Y., 2015. Biocatalysis conversion of methanol to methane in an upflow anaerobic sludge blanket (UASB) reactor: Long-term performance and inherent deficiencies. Bioresour. Technol. 198 691-700.

Lu, X., Zhen, G., Ni, J., Kubota, K., Li, Y.Y., 2017. Sulfidogenesis process to strengthen re-granulation for biodegradation of methanolic wastewater and microorganisms evolution in an UASB reactor. Water Res. 108, 137-150.

Luo, Q.S., Wang, H., Zhang, X.H., Qian, Y., 2005. Effect of direct electric current on the cell surface properties of phenol-degrading bacteria. Appl. Environ. Microbiol. 71, 423-427.

Marone, A., Carmona-Martinez, A.A., Sire, Y., Meudec, E., Steyer, J.P., Bernet, N., Trably, E., 2016. Bioelectrochemical treatment of table olive brine processing wastewater for biogas production and phenolic compounds removal. Water Res. 100, 316-325.

McSwain, B.S., Irvine, R.L., Hausner, M., Wilderer, P.A., 2005. Composition and distribution of extracellular polymeric substances in aerobic flocs and granular sludge. Appl. Environ. Microbiol. 71, 1051-1057.

Mikkelsen, L.H., Keiding, K., 2002. Physico-chemical characteristics of full scale sewage sludges with implications to dewatering. Water Res. 36, 2451-2462.

Nishio, N., Silveira, R.G., Hamato, K., Nagai, S., 1993. High-rate methane production in a UASB reactor fed with methanol and acetate. J. Ferment. Bioeng. 75, 309-313.

Paulo, P.L., Stams, A.J.M., Field, J.A., Dijkema, C., Lier, J.B.V., Lettinga, G., 2003. Pathways of methanol conversion in a thermophilic anaerobic (55 °C) sludge consortium. Appl. Environ. Biotechnol. 63, 307-314.

Paulo, P.L., Vallero, M.V.G., Treviño, R.H.M., Lettinga, G., Lens, P.N.L., 2004. Thermophilic (55 ^{0}C) conversion of methanol in methanogenic-UASB reactors: influence of sulphate on methanol degradation and competition. J. Biotechnol. 111, 79-88.

Raskin, L., Poulsen, L.K., Noguera, D.R., Rittmann, B.E., Stahl, D.A., 1994. Quantification of methanogenic groups in anaerobic biological reactors by oligonucleotide probe hybridization. Appl. Environ. Microbiol. 60, 1241-1248.

Sasaki, K., Morita, M., Sasaki, D., Hirano, S., Matsumoto, N., Watanabe, A., Ohmura, N., Igarashi, Y., 2011. A bioelectrochemical reactor containing carbon fiber textiles enables efficient methane fermentation from garbage slurry. Bioresour. Technol. 102, 6837-6842.

Shen, C.F., Kosaric, N., Blaszczyk, R., 1993. The effect of selected heavy metals (Ni, Co and Fe) on anaerobic granules and their extracellular polymeric substances (EPS). Water Res. 27, 25-33.

Shen, J., Xu, X., Jiang, X., Hua, C., Zhang, L., Sun, X., Li, J., Mu, Y., Wang, L., 2014. Coupling of a bioelectrochemical system for p-nitrophenol removal in an upflow anaerobic sludge blanket reactor. Water Res. 67, 11-18.

van Eerten-Jansen, M.C.A.A., Jansen, N.C., Plugge, C.M., de Wilde, V., Buisman, C.J.N., ter Heijne, A., 2015. Analysis of the mechanisms of bioelectrochemical methane production by mixed cultures. J. Chem. Technol. Biot. 90, 963-970.

Vlyssides, A., Barampouti, E.M., Mai, S., 2009. Influence of ferrous iron on the granularity of a UASB reactor. Chem. Eng. J. 146, 49-56.

Wang, K., Sheng, Y.X., Cao, H.B., Yan, K.P., Zhang, Y., 2017. Impact of applied current on sulfate-rich wastewater treatment and microbial biodiversity in the cathode chamber of microbial electrolysis cell (MEC) reactor. Chem. Eng. J. 307, 150-158.

Yu, H.Q., Fang, H.H.P., Tay, J.H., 2000. Effects of Fe^{2+} on sludge granulation in upflow anaerobic sludge blanket reactors. Water Sci. Technol. 41, 199-205.

Zhang, J.X., Zhang, Y.B., Quan, X., Chen, S., 2015. Enhancement of anaerobic acidogenesis by integrating an electrochemical system into an acidogenic reactor: Effect of hydraulic retention times (HRT) and role of bacteria and acidophilic methanogenic Archaea. Bioresour. Technol. 179, 43-49.

Zhao, Z., Zhang, Y., Chen, S., Quan, X., Yu, Q., 2014. Bioelectrochemical enhancement of anaerobic methanogenesis for high organic load rate wastewater treatment in a up-flow anaerobic sludge blanket (UASB) reactor. Sci. Rep. 4, 6658.

Zhen, G., Kobayashi, T., Lu, X., Kumar, G., Xu, K.Q., 2016a. Biomethane recovery from Egeria densa in a microbial electrolysis cellassisted anaerobic system: Performance and stability assessment. Chemosphere 149, 121-129.

Zhen, G., Kobayashi, T., Lu, X., Xu, K.Q., 2015. Understanding methane bioelectrosynthesis from carbon dioxide in a twochamber microbial electrolysis cells (MECs) containing a carbon biocathode. Bioresour. Technol. 186, 141-148.

Zhen, G., Lu, X., Kobayashi, T., Kumar, G., Xu, K.Q., 2016b. Promoted electromethanosynthesis in a two-chamber microbial electrolysis cells (MECs) containing a hybrid biocathode covered with graphite felt (GF). Chem. Eng. J. 284 1146-1155.

Zhen, G., Lu, X., Li, Y.Y., Zhao, Y.C., 2014. Combined electrical-alkali pretreatment to increase the anaerobic hydrolysis rate of waste activated sludge during anaerobic digestion. Appl. Energ. 128, 93-102.

Zhen, G., Lu, X., Li, Y.Y., Zhao, Y.C., 2013. Innovative combination of electrolysis and Fe(II)-activated persulfate oxidation for improving the dewaterability of waste activated sludge. Bioresour. Technol. 136, 654-663.

615 Zhen, G., Lu, X., Li, Y.Y., Zhao, Y.C., Wang, B., Song, Y., Chai, X.L., Niu, D.J., Cao, X.Y., 2012a.
616 Novel insights into enhanced dewaterability of waste activated sludge by Fe(II)-activated persulfate
617 oxidation. Bioresour. Technol. 119, 7-14.
618 Zhen, G., Takuro, K., Lu, X., Kumar, G., Hu, Y., Bakonyi, P., Rozsenberszki, T., Kook, L.,
619 Nemestothy, N., Belafi-Bako, K., Xu, K., 2016c. Recovery of biohydrogen in a single-chamber
620 microbial electrohydrogenesis cell using liquid fraction of pressed municipal solid waste (LPW) as
621 substrate. Int. J. Hydrogen Energy 41, 17896-17906.
622 Zhen, G., Lu, X., Wang, B.Y., Zhao, Y.C., Chai, X.L., Niu, D.J., Zhao, A.H., Li, Y.Y., Song, Y., Cao,
623 X.Y., 2012b. Synergetic pretreatment of waste activated sludge by Fe (II)–activated persulfate
624 oxidation under mild temperature for enhanced dewaterability. Bioresour. Technol. 124, 29-36.
625 Zhou, W.L., Imai, T., Ukita, M., Li, F.S., Yuasa, A., 2007. Effect of loading rate on the granulation
626 process and granular activity in a bench scale UASB reactor. Bioresour. Technol. 98, 1386-1392.

627

628

629

Figure Captions:

Fig. 1. Schematic diagram and photos of the UASB and combined UASB-MEC reactors.

Fig. 2. Current generation (a) and methane content (b) and production rate (c).

Fig. 3. Variations in pH, TS, VS, TCOD and SCOD of the effluent.

Fig. 4. S-EPS, LB-EPS and TB-EPS contents and PN/PS ratio in the granules sampled from the single UASB and the combined UASB-MEC reactors.

Fig. 5. SEM images of the granules collected, respectively, from the single UASB (a) and the UASB-MEC (b) reactors at the end of experiments.

Fig. 6. Microbial cells identified by Fluorescence *in-situ* hybridization (FISH) analysis in the single UASB (a), and UASB-MEC system (b). Total cells identified with DAPI stain (blue), *Archaea* hybridizing with Cy3-labeled ARC915 probe (red), and *Bacteria* hybridizing with Cy3-labeled EUB338 probe (red). (For interpretation of the references to colour in this figure legend, the reader is referred to the web version of this article.)

Fig. 7. Degradation routes of methanol involved within the normal UASB and UASB-MEC system.

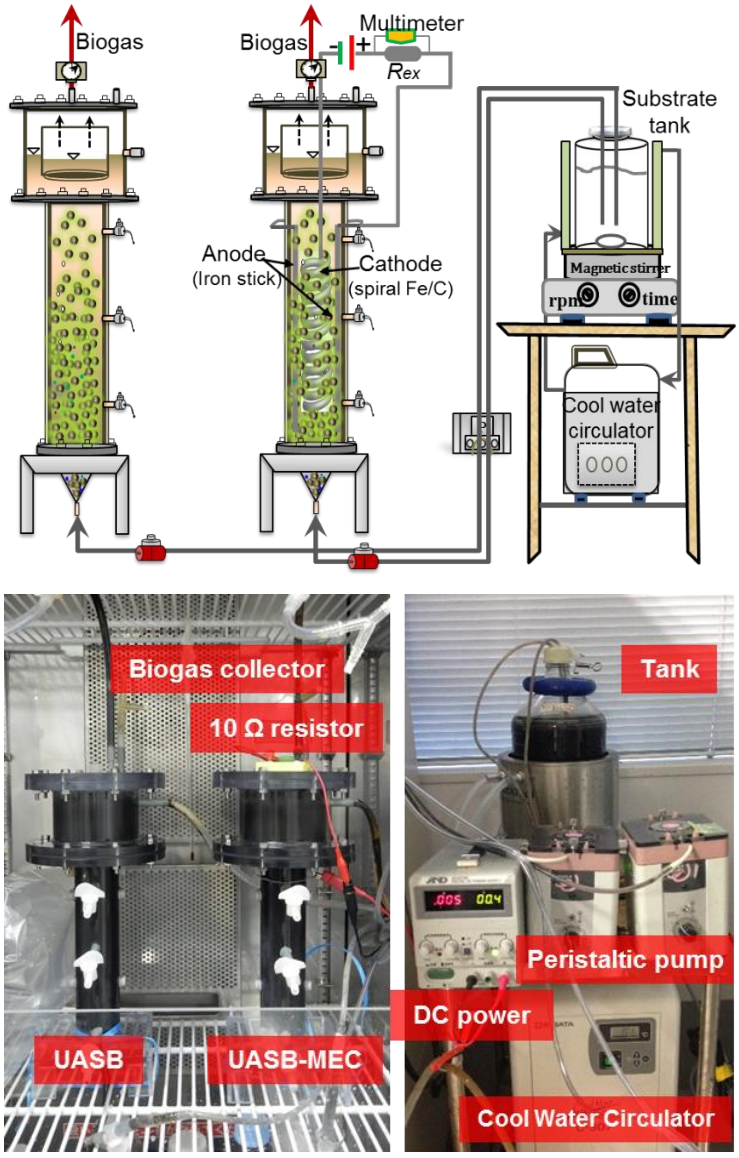
Biogas
Biogas
Multimeter
Rex
Substrate tank
Anode
(Iron stick)
Cathode
(spiral Fe/C)
Magnetic stirrer
rpm
time
Cool water circulator
Biogas collector
10 Ω resistor
UASB
UASB-MEC
Tank
Peristaltic pump
DC power
Cool Water Circulator

Fig. 1.

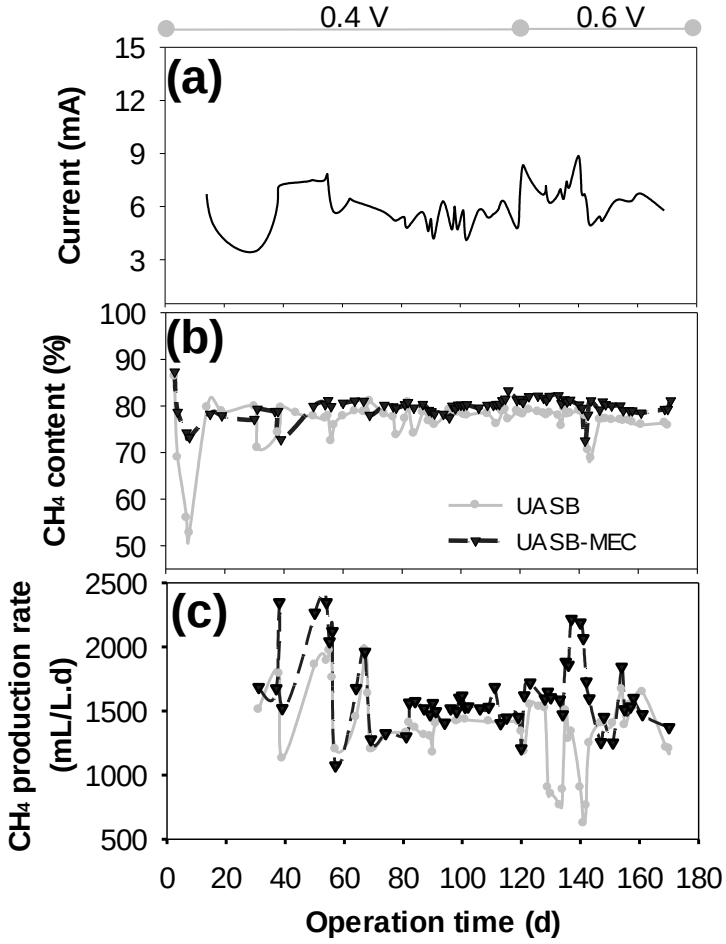
0.4 V
0.6 V
(a)
Current (mA)
15
12
9
6
3
(b)
CH4 content (%)
100
90
80
70
60
50
UASB
UASB-MEC
(c)
CH4 production rate (mL/L.d)
2500
2000
1500
1000
500
0
20
40
60
80
100
120
140
160
180
Operation time (d)

Fig. 2.

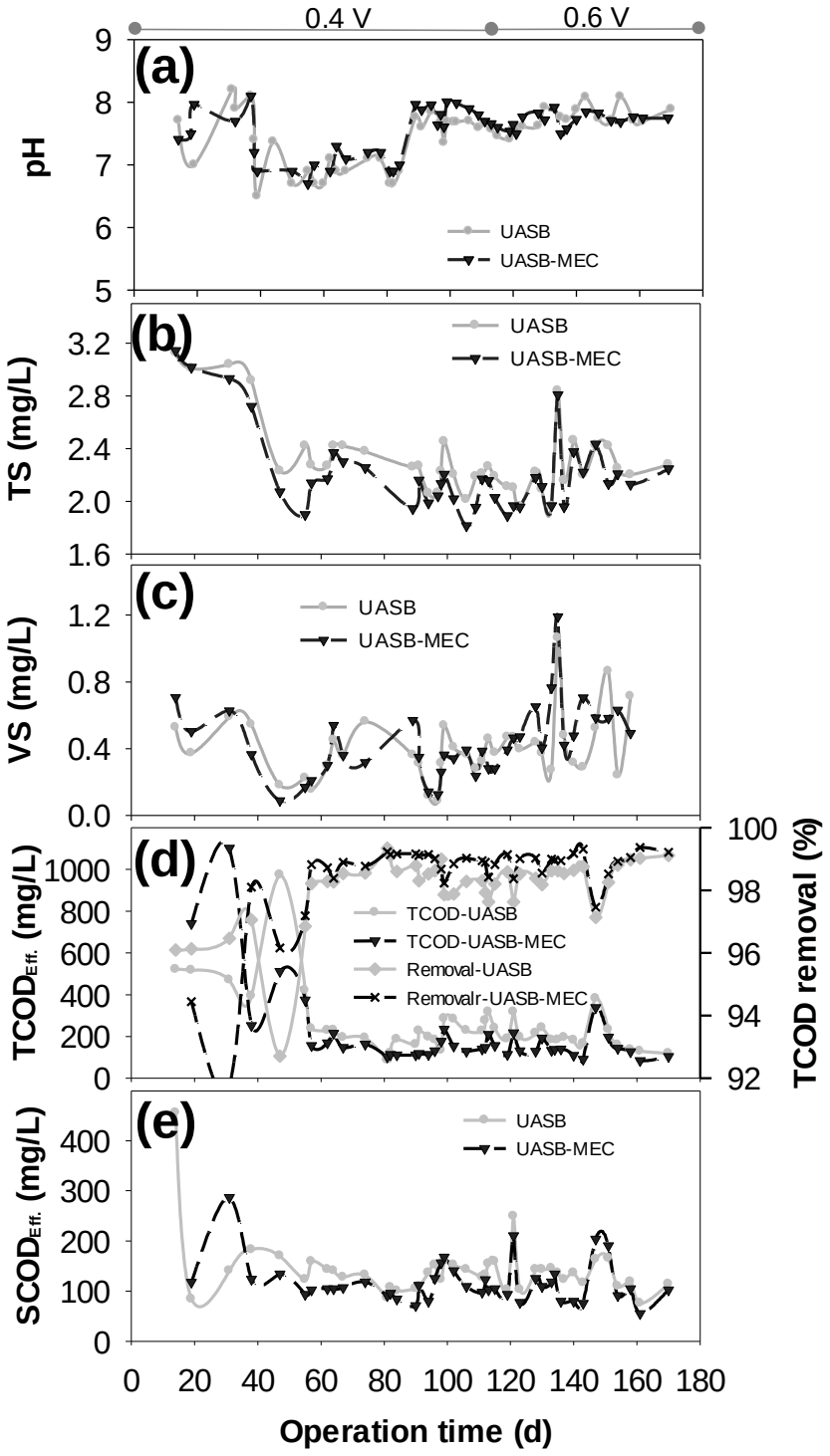
0.4 V
0.6 V
(a)
pH
UASB
UASB-MEC
(b)
TS (mg/L)
(c)
VS (mg/L)
(d)
TCOD-UASB
TCOD-UASB-MEC
Removal-UASB
Removalr-UASB-MEC
TCOD removal (%)
(e)
SCOD Eff. (mg/L)
Operation time (d)

Fig. 3.

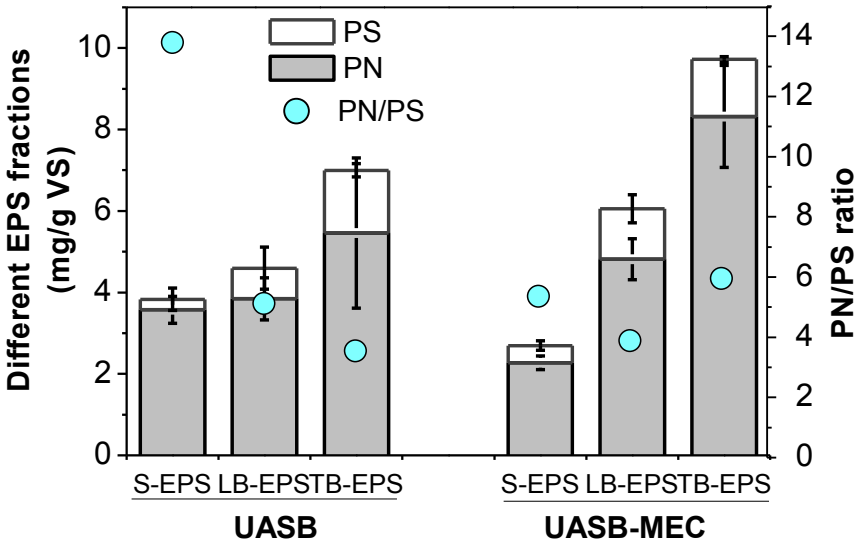
PS
PN
PN/PS
Different EPS fractions (mg/g VS)
PN/PS ratio
0
2
4
6
8
10
12
14
S-EPS LB-EPS TB-EPS
S-EPS LB-EPS TB-EPS
UASB
UASB-MEC

Fig. 4.

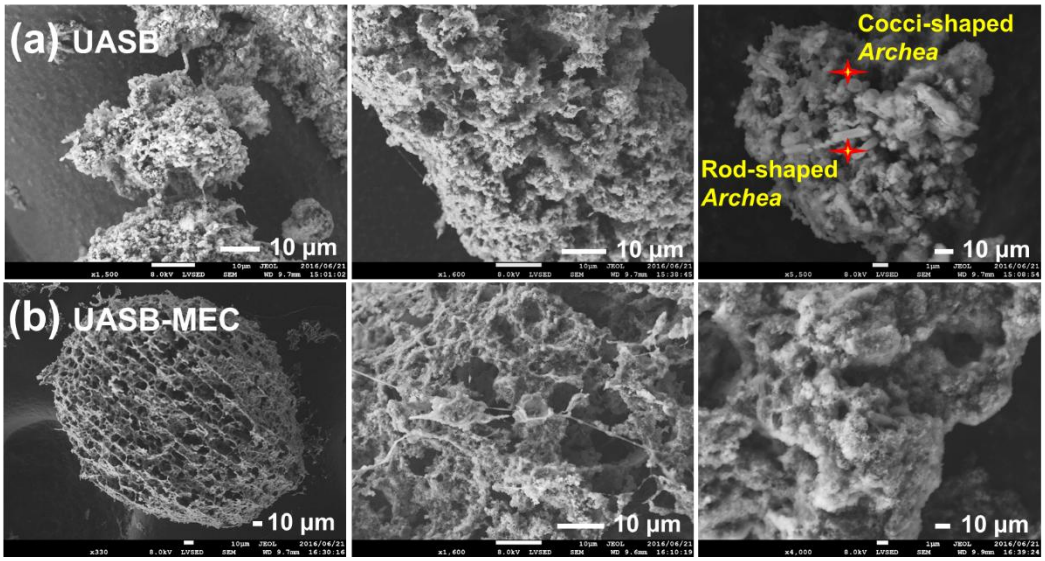
(a) UASB
10 μm
10 μm
Cocci-shaped
Archea
Rod-shaped
Archea
10 μm
(b) UASB-MEC
10 μm
10 μm
10 μm

Fig. 5.

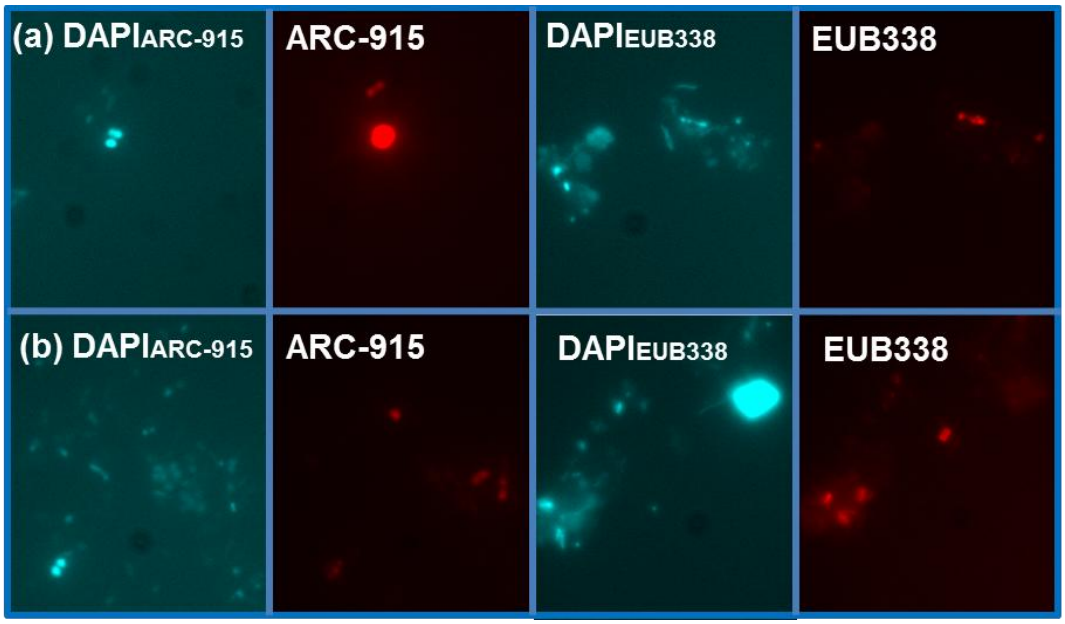
(a) DAPIARC-915
ARC-915
DAPIEUB338
EUB338
(b) DAPIARC-915
ARC-915
DAPIEUB338
EUB338

Fig. 6.

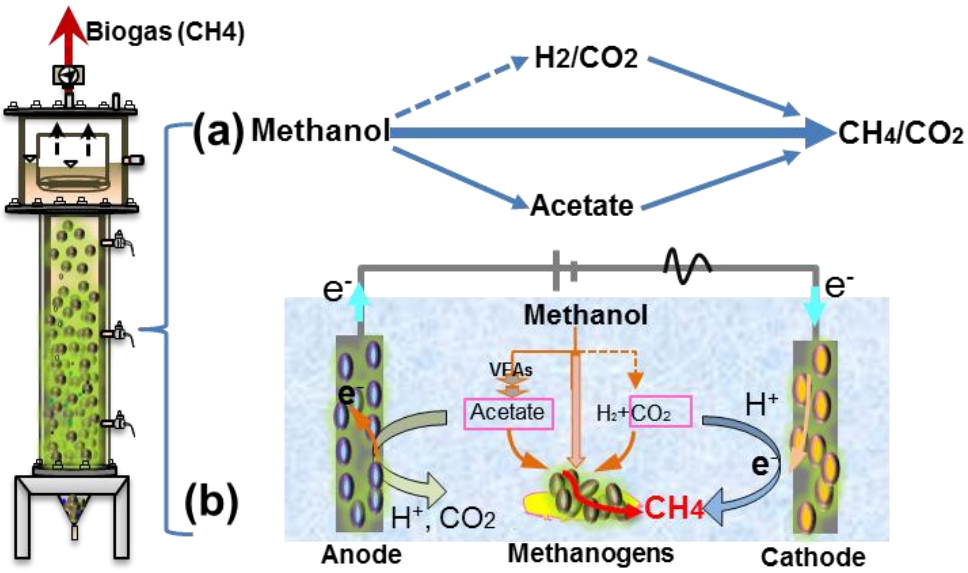
Biogas (CH4)
(a)
Methanol
H2/CO2
CH4/CO2
Acetate
(b)
e-
e-
Methanol
VFAs
Acetate
H2+CO2
H+
e-
e-
H+, CO2
CH4
Anode
Methanogens
Cathode

Fig. 7.